Article

Neuron

Loss of Striatonigral GABAergic Presynaptic Inhibition Enables Motor Sensitization in Parkinsonian Mice

Highlights

- Dopamine denervation enables sensitized striatonigral-mediated motor activation
- Dopamine denervation leads to increased striatonigral synaptic activity
- Striatonigral GABA release is controlled by $GABA_B$ autoreceptors
- Dopamine denervation disrupts normal $GABA_B$-mediated control of striatonigral activity

Authors

Anders Borgkvist, Elizabeth M. Avegno, Minerva Y. Wong, ..., Mark S. Sonders, Rene Hen, David Sulzer

Correspondence

ds43@cumc.columbia.edu

In Brief

In Parkinson's disease patients, dopamine replacement therapy eventually triggers sensitized and uncontrolled motor responses. Borgkvist et al. reveal a dopamine-independent role for elevated presynaptic transmission at striatonigral GABA synapses in parkinsonian motor sensitization.

Borgkvist et al., 2015, Neuron *87*, 976–988
September 2, 2015
http://dx.doi.org/10.1016/j.neuron.2015.08.022

CellPress

CellPress

Neuron
Article

Loss of Striatonigral GABAergic Presynaptic Inhibition Enables Motor Sensitization in Parkinsonian Mice

Anders Borgkvist,[1] Elizabeth M. Avegno,[2] Minerva Y. Wong,[2] Mazen A. Kheirbek,[3] Mark S. Sonders,[1,3] Rene Hen,[4] and David Sulzer[1,2,3,5,*]
[1]Department of Neurology
[2]Department of Pharmacology
[3]Department of Psychiatry
[4]Department of Neuroscience
Columbia University, New York, NY 10032, USA
[5]New York State Psychiatric Institute, New York, NY 10032, USA
*Correspondence: ds43@cumc.columbia.edu
http://dx.doi.org/10.1016/j.neuron.2015.08.022

SUMMARY

Degeneration of dopamine (DA) neurons in Parkinson's disease (PD) causes hypokinesia, but DA replacement therapy can elicit exaggerated voluntary and involuntary behaviors that have been attributed to enhanced DA receptor sensitivity in striatal projection neurons. Here we reveal that in hemiparkinsonian mice, striatal D1 receptor-expressing medium spiny neurons (MSNs) directly projecting to the substantia nigra reticulata (SNr) lose tonic presynaptic inhibition by $GABA_B$ receptors. The absence of presynaptic $GABA_B$ response potentiates evoked GABA release from MSN efferents to the SNr and drives motor sensitization. This alternative mechanism of sensitization suggests a synaptic target for PD pharmacotherapy.

INTRODUCTION

The motor symptoms in Parkinson's disease (PD) are caused by the loss of dopamine (DA) neurons of the substantia nigra pars compacta (SNc) (Fahn, 2000), as shown by the success of replacement therapy with the DA precursor 3,4-dihydroxy-L-phenylalanine (L-DOPA). L-DOPA therapy, however, also generates excessive behavioral responses to environmental stimuli (Weintraub and Nirenberg, 2013), impulse control disorders (Voon et al., 2011), and dyskinesias (Fahn, 2000).

Studies using animal models of PD indicate that L-DOPA and DA receptor agonists cause sensitized motor behavior due to a denervation-induced supersensitivity of DA receptors (Marshall and Ungerstedt, 1977). These responses can occur following the first administration of DAergic drugs to DA-depleted animals (Putterman et al., 2007), indicating that the DA denervation is itself sufficient to induce abnormal behavioral responses to drug treatment. Indeed, dyskinesia appears rapidly in patients with a late diagnosis of PD, and in individuals with acute parkinsonism from the neurotoxin MPTP (Langston and Ballard, 1984) or inherited defects in DA synthesis (Pons et al., 2013). These observations reinforce the hypothesis that adaptations to low DA signaling contribute to the expression of side effects of L-DOPA therapy (Nadjar et al., 2009). L-DOPA administration, however, influences subsequent behavioral responses to the drug (Morelli et al., 1989), and the impact of the adaptations established without DA replacement therapy is unknown.

The striatal GABAergic medium spiny projection neurons that are enriched in DA D1 receptors (D1R) play a central role in the expression of sensitization to L-DOPA in DA denervated animals (Feyder et al., 2011). The D1-MSNs give rise to the striatonigral "direct pathway," sending long-range axons to the GABAergic neurons of the substantia nigra pars reticulata (SNr) (Gerfen, 1992). Motor-stimulating striatonigral activation pauses SNr tonic firing, disinhibiting their target nuclei in the thalamus, brainstem, and superior colliculus (Deniau et al., 2007). The idea that DA denervation elicits sensitization to L-DOPA in part via stimulation of the striatonigral pathway is supported by observations that DA denervated animals exhibit increased D1R-mediated release of GABA within the SNr (Mango et al., 2014; Rangel-Barajas et al., 2008). In addition, homeostatic changes driven by the absence of DA lead to increased excitability of D1-MSNs, which is not normalized by L-DOPA (Fieblinger et al., 2014; Warre et al., 2011), indicating that adaptive responses extend beyond activation of D1Rs. Whether these changes are reflected in neurotransmitter release from striatonigral synapses in the SNr and if they are sufficient to affect behavior are unknown.

Here, we circumvented DA D1R stimulation of striatonigral activity in DA lesioned mice using optogenetics. To measure changes in neurotransmitter release from striatonigral terminals subsequent to nigrostriatal DA lesion, we used patch-clamp recordings and developed an optical approach to measure presynaptic activity in the SNr using the fluorescent synaptic vesicle endocytic probe FM1-43 (Betz and Bewick, 1992). Our data demonstrate that DA denervation increases the probability of synaptic vesicle fusion and GABA release from striatonigral synapses, presumably as a compensatory response; that the increased presynaptic input is due to reduced $GABA_B$ autoreceptor responses; and that changes in basal ganglia circuitry that can elicit behavioral sensitization occur presynaptically at

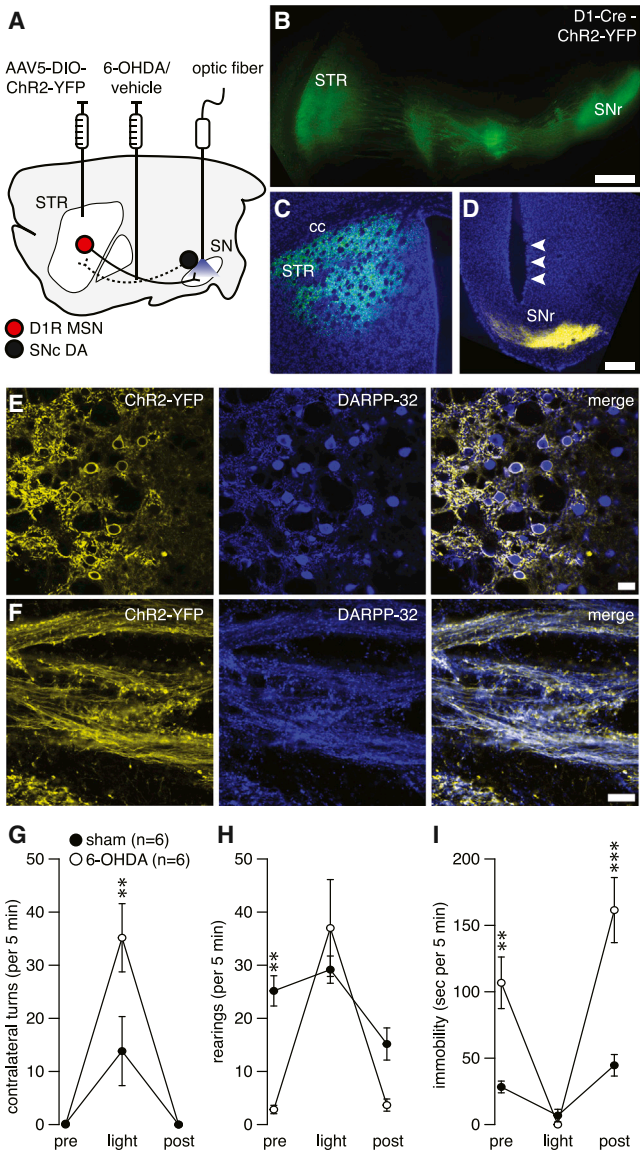

Figure 1. Optogenetic Stimulation of Striatonigral Synapses Reduces Hypokinesia and Reveals a Supersensitive Direct Pathway in 6-OHDA Lesioned Mice

(A) Schematic of a sagittal brain slice indicating AAV5-DIO-ChR2-eYFP and 6-OHDA injection sites and the fiber optic placement. STR, striatum; SN, substantia nigra.

(B) Oblique (10°) sagittal section showing the Cre-dependent expression of ChR2-eYFP in the striatonigral pathway 3 weeks after AAV injection into BAC transgenic D1R-Cre mice (scale, 1 mm).

(C and D) Coronal section of (C) the dorsal striatum and (D) the SNr showing ChR2-eYFP (yellow) and DAPI (blue) fluorescence. cc, corpus callosum. The track of the fiber optic is outlined with arrowheads in (D) (scale, 200 μm).

(E and F) (E) Confocal micrographs of ChR2-eYFP, DARPP-32 immunoreactivity, and the colocalization of the two signals in the striatum, and (F) within striatonigral fibers rostral to the SNr.

(G–I) Effect of illuminating the SNr with flashes (5 ms) of blue light (10 Hz; 5 min) on (G) the number of 360° contralateral turns (H) number of rearings and (I) the time (in seconds) spent in immobility. *p < 0.05; **p < 0.01; ***p < 0.001 (two-way analysis of variance (ANOVA), Tukey's test). n = 6 mice per group. Mean ± SEM (see also Figures S2 and S3).

MSN axons within the SNr and are independent of DA receptor stimulation.

RESULTS

We injected 6-OHDA or vehicle unilaterally into the medial forebrain bundle, which contains the ascending nigrostriatal DA projections, and confirmed contralateral sensorimotor deficits ~3 weeks later in the corridor test (Grealish et al., 2010). As sensitization to L-DOPA is observed with severe DA denervation (Putterman et al., 2007), this paradigm was used to select mice with an impairment which corresponds to >80% loss of striatal DA innervation (Grealish et al., 2010) (see Figures S1A–S1D available online). We confirmed that 6-OHDA decreased tyrosine hydroxylase and dopamine transporter proteins in the striatum (Figures S1E–S1G).

Expression of ChR2 in the Striatonigral Pathway

To examine striatonigral function in vivo, we administered adeno-associated virus encoding channelrhodopsin-2 fused to enhanced yellow fluorescent protein (AAV5-DIO-ChR2-eYFP) into ipsilateral dorsal striatum of 6-OHDA and sham-treated transgenic mice expressing Cre recombinase under control of the D1R promoter (Figure 1A). An optical fiber was implanted dorsal to the SNr to activate striatonigral efferents. Examination of ChR2-eYFP expression was carried out in striatum and SNr 3–4 weeks after surgery (Figures 1B–1F). ChR2-eYFP was found in neurons that expressed DARPP-32 (Figure 1E), but not *met*-enkephalin (Figures S2A–S2C), a selective marker for striatopallidal MSNs (Gerfen et al., 1990). Furthermore, ChR2-eYFP was not found in cells expressing choline acetyltransferase, parvalbumin, neuropeptide Y and calretinin (Figures S2D–S2I; Table S1), verifying that ChR2 was excluded from striatal interneurons and that ChR2 was confined to striatonigral MSNs. Consistently, ChR2-eYFP was expressed by DARPP-32-positive rostrocaudal projection fibers and terminal fields within the SNr, confirming the anterograde transport of ChR2 to striatonigral axon terminals (Figure 1F).

Effect of Selective Stimulation of Striatonigral Synapses

Unilateral inhibition of the postsynaptic neurons in the SNr by GABA agonists leads to dose-dependent contralateral turning behavior in rodents (Waddington and Cross, 1979). We hypothesized that the number of contralateral turns would correspond to inhibition driven by striatonigral GABA release.

Selective stimulation of striatonigral synapses by illumination of the ipsilateral SNr with flashes (5 ms, 5 min at 10 Hz) of blue light produced a greater behavioral response in DA denervated mice, as measured by the number of contralateral turns performed and forward locomotion (Figures 1G and S2J–S2L; Movie S1 and Movie S2). In the absence of optogenetic stimulation, 6-OHDA-treated mice reared to explore the environment infrequently (Figure 1H) and spent more time immobile (Figure 1I) than sham-treated controls. These hypokinetic phenotypes were reduced by optogenetic stimulation of the striatonigral terminals in the SNr. The behavioral responses were time-locked to the striatonigral activation, as rotational behavior, the frequency of rearing, and the time spent immobile

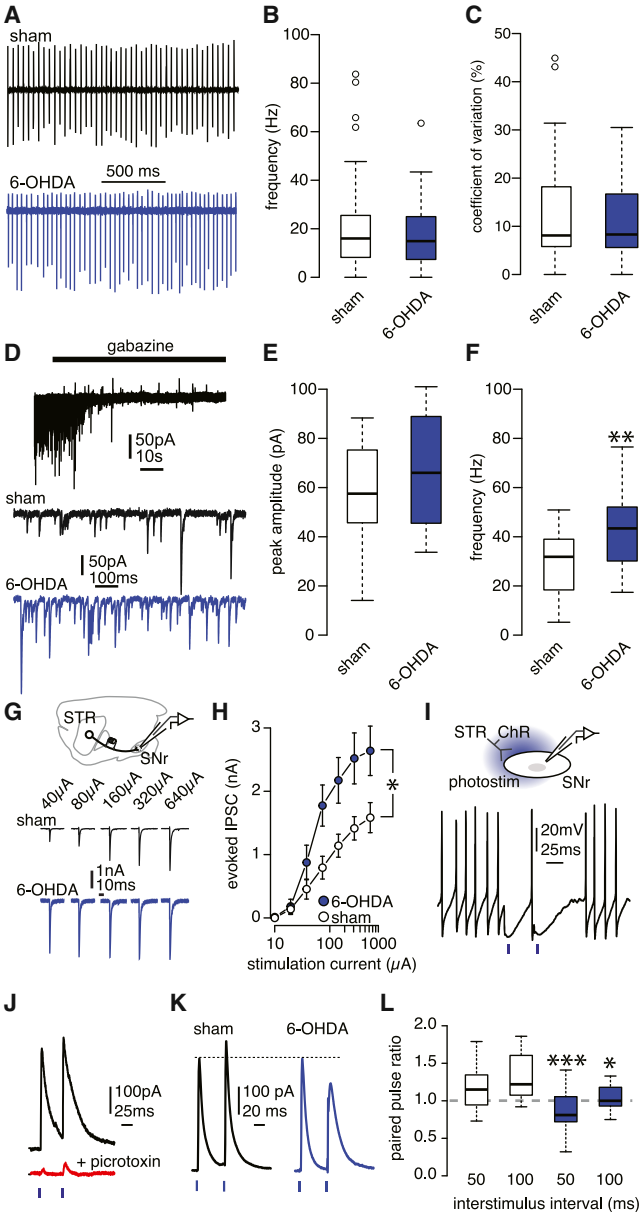

Figure 2. Increased Striatonigral GABA Transmission in 6-OHDA Lesioned Mice

(A) Cell-attached recordings from SNr neurons in brain slices from sham (black) and 6-OHDA lesioned mice (blue).

(B and C) (B) Frequency and (C) coefficient of variation of SNr action currents in cell-attached recordings from sham (n = 57 cells; 12 mice) and 6-OHDA (n = 44 cells; 11 mice) slices.

(D) sIPSCs recorded in SNr neurons of sham animals (top and middle) during bath application of the $GABA_A$ antagonist gabazine (10 μM) (top), and in a SNr neuron of a 6-OHDA lesioned mouse (bottom, blue).

(E and F) (E) Amplitude and (F) frequency of sIPSCs recorded in sham (white; n = 22 cells; 8 mice) and 6-OHDA lesioned mice (blue, n = 27 cells; 11 mice). **p < 0.01, t test.

(G) Schematic of the brain slice configuration used to record electrically evoked striatonigral GABA currents in whole-cell patch clamp (top). IPSCs recorded from SNr neurons at increasing stimulation current applied to the striatonigral fibers in slices from sham (black) and 6-OHDA (blue)-treated mice (bottom).

(H) IPSC peak amplitudes as a function of stimulation current in slices from sham (n = 18 cells, 7 mice) and 6-OHDA (n = 20 cells, 10 mice) treated mice. *p < 0.05 (two-way ANOVA, Tukey's test). Mean ± SEM.

(I) Schematic of the brain slice configuration used to record optically evoked striatonigral GABA currents in whole-cell patch clamp (top panel). ChR2-evoked inhibition (2 × 1 ms blue flash indicated) of a SNr neuron recorded in current clamp (bottom panel).

(J) ChR2-evoked picrotoxin-sensitive $GABA_A$ currents in voltage-clamped SNr neurons. Note the pronounced PPF in response to the two flashes (0.5 ms; 50 ms ITI) of blue light.

(K) ChR2-evoked IPSCs recorded in SNr neurons in slices from sham (black) and 6-OHDA (blue) lesioned mice. Responses are scaled to the initial IPSCs.

(L) The paired-pulse ratio of optically evoked IPSCs recorded in SNr neurons from sham (white; n = 16 cells, 7 mice at 50 ms ITI and n = 12 cells, 6 mice at 100 ms ITI) and 6-OHDA (blue; n = 15 cells, 6 mice at 50 ms ITI and n = 9 cells, 6 mice at 100 ms ITI) lesioned mice. *p < 0.05, ***p < 0.001, t test (see also Figure S4).

returned to prestimulus levels when illumination of the SNr was terminated.

Stimulation of the SNr did not induce expression of c-Fos, an indirect marker for neuronal activity, in MSN cell bodies (Figures S3A and S3B), suggesting that the behavioral effect did not involve striatal activation. We found no correlation between the ChR2 expression level and the number of rotations performed by the same animal (Figure S3C), confirming that the DA denervation, not the ChR2 expression level, was responsible for the increased behavioral response observed.

In summary, direct stimulation of the striatonigral synapse promotes locomotion in 6-OHDA lesioned mice, and chronic loss of DA leads to a sensitized behavioral response to striatonigral activation.

Effect of Dopamine Loss on SNr GABA Transmission

To explore how striatonigral activation leads to sensitized behavior in DA-depleted mice, we prepared oblique acute sagittal brain slices containing the striatum, the striatonigral fibers, and the SNr (Figure 2G). Cell-attached recordings from principal GABAergic SNr neurons (Figures S4A–S4E) revealed no differences in firing frequency or pattern of activity (Figures 2A–2C; $p > 0.05$, Wilcox test), determined as the coefficient of variation, between DA denervated cells and control mice.

To measure presynaptic function, we recorded spontaneous synaptic inputs in the presence of NBQX (10 μM) and AP5 (50 μM) to block glutamatergic responses by AMPA and NMDA receptors, respectively, and loaded SNr neurons with 144 mM chloride in the pipette solution to facilitate detection of spontaneous inhibitory postsynaptic currents (sIPSCs). At –60 mV holding potential, we observed inward currents that were blocked by the $GABA_A$ receptor antagonist gabazine (10 μM), confirming their identity as $GABA_A$-mediated sIPSCs (Figure 2D). No differences were observed in the amplitude of sIPSCs between sham and 6-OHDA lesioned animals, but there was an increased frequency of sIPSCs in 6-OHDA lesioned mice (Figures 2E and 2F). As changes in the frequency of spontaneous synaptic events are generally considered to reflect presynaptic modifications in synaptic strength, these results provided a first indication that DA denervation increased GABA transmission in the SNr by presynaptic enhancement of GABA release.

The sIPSCs recorded in SNr neurons are presumably due to a combination of $GABA_A$ currents elicited by striatonigral, pallidonigral, and local SNr inputs (Deniau et al., 1982; von Krosigk et al., 1992). In the majority of SNr neurons (53/71) held at –60 mV with 16 mM Cl^- in the pipette solution, distal stimulation of SNr afferents evoked outward $GABA_A$-mediated IPSCs (Figures S4F–S4H), with properties equivalent to striatonigral synapses (Figure S4I) (Connelly et al., 2010; Miyazaki and Lacey, 1998). These currents were identical to the optogenetically evoked striatonigral IPSCs (Figure 2J). In a smaller fraction of SNr cells (18/71), we observed inward $GABA_A$ currents with properties similar to pallidonigral inputs (Figures S4F–S4H) (Connelly et al., 2010; Miyazaki and Lacey, 1998). For the majority of these cells (13/18), the inward current was followed by an outward current (Figure S4F), consistent with observations that SNr neurons receive convergent inputs from the globus pallidus (GP) and striatum (von Krosigk et al., 1992). The putative striatonigral synapses were characterized by longer delay after stimulation, slower kinetics, and facilitation in response to paired pulse stimuli (Figure S4I; 50 ms interstimulus interval, ITI). Thus, electrical stimulation evokes striatonigral and occasionally pallidonigral GABA release; pallidonigral synapses appear to exhibit distinct electrophysiological properties including inward currents and short delay, providing a means to isolate the apparent striatonigral component on cells that received both inputs.

To examine differences in striatonigral input between sham and 6-OHDA lesioned mice, we used electrical stimulus and optogenetics (Figures 2G–2I). In SNr neurons filled with high Cl^- (144 mM) to increase detection of GABA release, electrical stimulation evoked IPSCs with striatonigral properties in both groups, as indicated by the delay after stimulation (sham, 6.4 ± 0.6 ms; 6-OHDA, 6.0 ± 0.3 ms, $p > 0.05$, t test) and the decay constant of the synaptic current (sham, 7.1 ± 0.8 ms, n = 18 cells; 6-OHDA, 9.3 ± 0.9 ms, $p > 0.05$, t test). We did not observe any putative pallidonigral currents. We found a gradual increase in the amplitude of the IPSCs with increasing current in both sham and 6-OHDA mice; however, consistent with a potentiated striatonigral pathway after DA denervation, the IPSCs were larger in the lesioned mice (Figures 2G and 2H).

In current clamp recordings from principal SNr GABA neurons, illumination of brain slices from D1-Cre-AAV-ChR2-eYFP mice with blue light (0.5–1 ms; Figure 2I) interrupted spontaneous activity, and in voltage clamp recordings, illumination elicited picrotoxin-sensitive (100 μM) $GABA_A$ receptor-mediated synaptic currents (Figure 2J). Thus, stimulation of striatonigral inputs caused GABA release that inhibited SNr tonic firing via activation of $GABA_A$ receptors.

We compared the short-term plasticity evoked by pairs of striatonigral photostimulation (Figures 2J and 2K). The paired-pulse ratio (PPR) of the second response to the first determines the initial release probability of synapses (Zucker and Regehr, 2002). Similar to electrical stimuli (Figure S4I), currents evoked by pairs of striatonigral photostimulation (50–100 ms ITI) in sham animals revealed that striatonigral synapses had low release probability, as indicated by pronounced PPF (Figures 2K and 2L). In contrast, stimuli applied to the SNr in 6-OHDA animals resulted in short-term plasticity representative of synapses with high release probability; we observed paired-pulse depression (PPD) at 50 ms ITI, with nearly identical currents in response to the first and second pulse with 100 ms paired-pulse photostimulation (Figure 2L). There was no rundown of evoked SNr currents over 5 min of continuous optical stimulation of the striatonigral fibers at 100 ms ITI (Figure S5), similar parameters to that used for behavioral experiments (cf. Figures 1 and S2). We found no clear PPD of IPSCs evoked by electrical stimulation (50 ms ITI) of the striatonigral fibers in DA denervated animals (cf. Figure 6F), while observing a significant reduction in PPF; the PPR was 1.27 ± 0.06, n = 11 cells and 1.09 ± 0.05, n = 7 cells ($p < 0.05$, t test) in sham and 6-OHDA lesioned mice, respectively. The differences between electrical and optical stimulation may be because electrical stimulation is less selective than optical stimulation or because ChR2 and AAVs used for gene delivery increase the release probability of synapses (Jackman et al., 2014; Zhang and Oertner, 2007).

Labeling of Striatonigral Synapses with FM1-43

The patch-clamp experiments suggested that the ability of the striatonigral pathway to elicit sensitized behaviors in parkinsonian animals was due to an increased release probability of GABA release from striatonigral synapses. Postsynaptic recordings, however, provide an indirect measure of presynaptic plasticity, and interpretation can be confounded by multiple postsynaptic mechanisms, including receptor expression, saturation, and desensitization. We therefore developed an optical approach using the dye FM1-43 to visualize the fusion of recycling synaptic vesicles at individual striatonigral synapses. FM1-43 acquires a bright fluorescent signal upon incorporation into the lipid bilayer of recycling synaptic vesicles (Betz and Bewick, 1992), and the release probability of individual release sites can be estimated by the rate of fluorescence decay during stimulus trains (Zakharenko et al., 2001).

To load FM1-43 into striatonigral synapses, we prepared sagittal slices and applied electrical stimulation to the striatonigral projection (Figures 3A and 3B), and then superfused ADVASEP-7 (100 μM) to remove unbound dye (Kay et al., 1999). Bright spherical fluorescent puncta with an average diameter of 0.69 ± 0.004 μm (n = 796) were revealed in the SNr by two-photon microscopy (Figures 3C and S6). Puncta were not present in slices exposed to FM1-43 in the absence of stimuli (Figure S7A).

FM1-43 unloading was achieved by a second round of stimulation (Figure 3C; Movie S3). When we severed the fibers with a knife cut after the loading stimulus, the puncta retained FM1-43 fluorescence during the stimuli (Figures S7B–S7E). In contrast, activity-dependent decrease in FM1-43 fluorescence was achieved by repositioning the stimulation electrode onto intact striatonigral fibers caudal to the knife cut (Figures S7B–S7E). Thus, loading and unloading of FM1-43 required intact projections from the striatum to the SNr.

To confirm that our FM1-43 loading procedure labeled striatonigral synapses, we used transgenic mice expressing tdTomato under control of the D1R promoter (Figures S7F–S7I), to transduce tdTomato fluorescence in D1-MSNs (Table S2). tdTomato expression within the SNr was confined to en passage fibers and DARPP-32 immunopositive profiles (Figure S7F). In contrast, SNr neurons visualized by Nissl stain did not contain

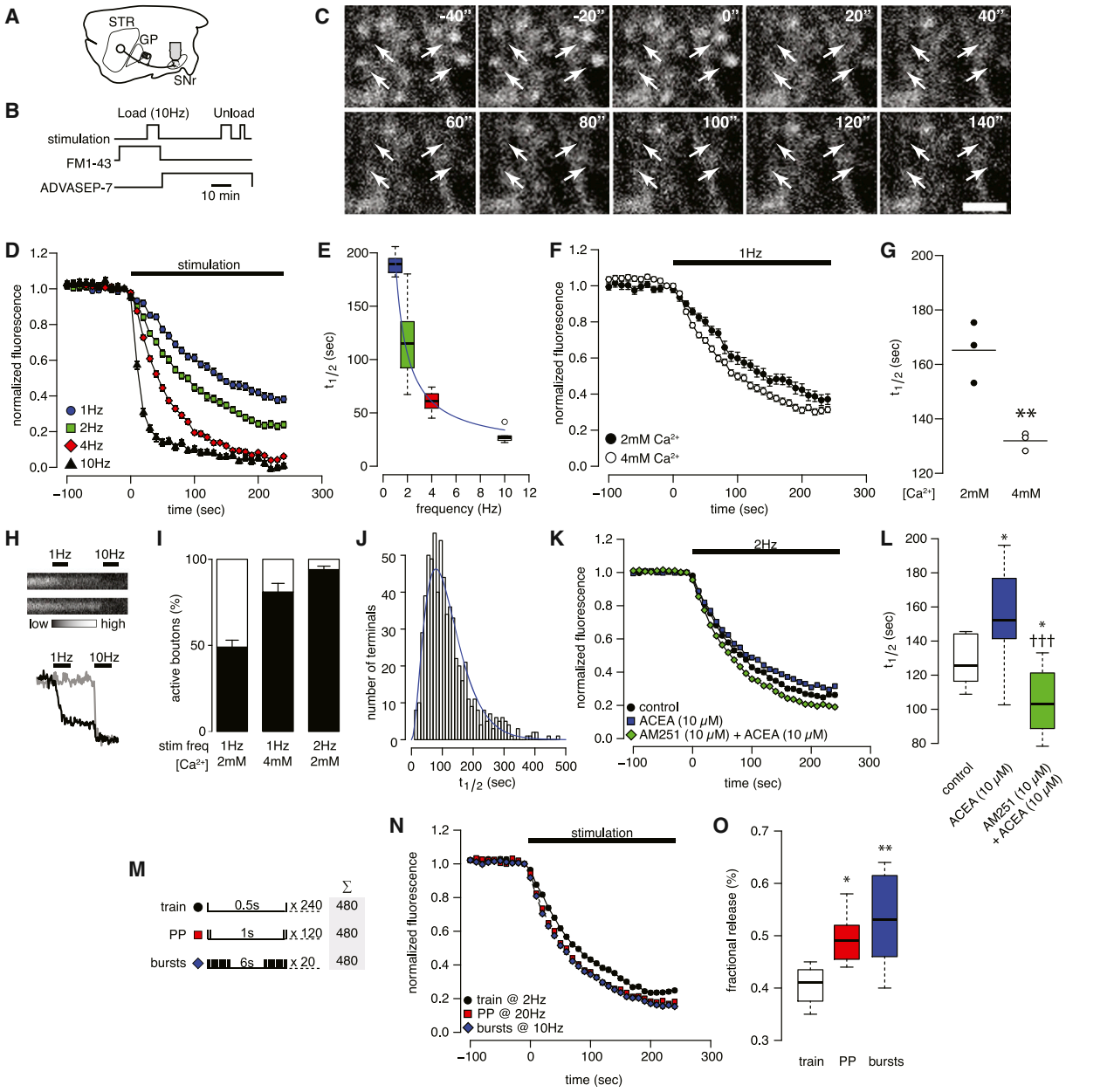

Figure 3. Two-Photon Imaging of FM1-43 Destaining Visualizes Vesicular Fusion at Individual Striatonigral Synaptic Boutons

(A) Schematic of a sagittal brain slice and placement of the stimulation electrode onto the striatonigral fibers. STR, striatum; GP, lateral globus pallidus; SNr, substantia nigra reticulata.

(B) Protocol for FM1-43 loading and unloading from striatonigral synapses.

(C) Two-photon images with FM1-43 labeled boutons (arrows) before (−40–0 s) and during (0–140 s) electrical stimulation (10 Hz) of the striatonigral pathway. The electrical stimulus began at 0. Scale, 3 μm.

(D) FM1-43 destaining from striatonigral synapses at 1 Hz (blue circles, n = 116 boutons; 9 slices), 2 Hz (green rectangles, n = 132 boutons; 5 slices), 4 Hz (red diamonds, n = 285 boutons; 11 slices), and 10 Hz (black triangles, n = 152 boutons; 6 slices) stimulus trains (mean ± SEM).

(E) Dependence of unloading on stimulation frequency. The data were fit by the equation $t_{1/2} = t_{1/2}$ (min) + q/f (Zakharenko et al., 2001), where $t_{1/2}$ is the half-time of unloading, $t_{1/2}$ (min) is the minimal half-time at 10 Hz frequency, f is the frequency of stimulation (Hz), and q is a constant. Mean ± SEM (n = 6–67 slices).

(F) FM1-43 destaining from striatonigral terminals in ACSF containing 2 mM (black, n = 38 terminals; 3 slices) or 4 mM Ca^{2+} (white, n = 137 terminals; 3 slices).

(G) Averaged $t_{1/2}$ at the different extracellular Ca^{2+} concentrations. Data represent mean $t_{1/2}$ per slice and line shows the group average. **p < 0.01, t test.

(H) Two-photon images of a 1 Hz destaining (upper) and 1 Hz nondestaining puncta (lower). Bottom panel shows the FM1-43 fluorescence of these two boutons.

(I) Ratio of the destaining puncta (filled) at the different extracellular Ca^{2+} concentrations and stimulation frequencies. Mean ± SEM per slice (n = 3–10 slices per condition).

(legend continued on next page)

tdTomato fluorescence. Virtually all FM1-43 puncta showing activity-dependent loss of fluorescence colocalized with tdTomato (97%, 131/134 puncta, n = 5 slices, 3 mice; Figures S7G–S7I), indicating that the majority of the FM1-43 fluorescent puncta colocalize with striatonigral projections.

FM1-43 destaining from each bouton is reported as the time required for the fluorescence intensity to decay to half of its initial value ($t_{1/2}$) (Figure S6; Supplemental Experimental Procedures). The rate of the stimulated FM1-43 destaining was dependent on the stimulus frequency and exhibited a pronounced slope between 1 Hz to 4 Hz (Figures 3D and 3E). Destaining of FM1-43, like neurotransmitter release, was dependent on Ca^{2+}, as addition of Cd^{2+} (200 μM) to the bath solution to block voltage-gated Ca^{2+} channels (VGCC) during unloading arrested exocytosis (Figure S6E). Consistently, enhancing extracellular Ca^{2+} from 2 mM to 4 mM caused more rapid destaining (Figures 3F and 3G).

With 1 Hz stimuli, a significant fraction of boutons maintained fluorescence (Figure 3H). We could increase the fraction of active boutons by increasing extracellular Ca^{2+} ($p < 0.001$, Fisher's exact test, n = 3 slices per group), or stimulating at 2 Hz ($p < 0.001$, Fisher's exact test, n = 9 slices per frequency): at the higher frequency, nearly all boutons exhibited stimulus-dependent FM1-43 destaining (Figure 3I). Thus, this optical approach identifies subsets of striatonigral synapses with a range of release probabilities. Consistent with multiple populations of striatonigral presynaptic sites, the frequency histogram (Figure 3J) at 2 Hz unloading stimuli revealed that the $t_{1/2}$ of the individual boutons diverged from a normal distribution ($p < 0.0001$, KS test, n = 665 boutons, 25 slices). We selected a stimulus frequency of 2 Hz, the point of highest slope and thus the dynamic range permitting optimal detection of changes in destaining (Figure 3E), for further analysis.

Regulation of FM1-43 Destaining by Cannabinoid Receptor 1 and Stimulus Pattern

To confirm that FM1-43 destaining provided a reliable measure of presynaptic striatonigral GABA transmission, we explored the influence of cannabinoid receptor 1 (CB1R), which is specifically expressed in the SNr by striatonigral efferents (Mátyás et al., 2006) and has been reported to inhibit striatonigral release (Wallmichrath and Szabo, 2002). Superfusion of FM1-43-loaded striatonigral synapses with the specific CB1R agonist ACEA (10 μM) decreased FM1-43 destaining during unloading (Figures 3K and 3L), an effect blocked by the CB1R antagonist, AM251 (10 μM). Indeed, the rate of destaining was decreased in the presence of AM251 below control, indicating that CB1Rs are tonically activated (Romo-Parra et al., 2009).

We then asked whether synaptic vesicle fusion exhibited short-term plasticity consistent with PPF in the electrophysiological recordings (cf. Figure 2). Following FM1-43 loading, the synapses were subjected to a range of stimulus patterns with an equivalent number of stimuli (Figure 3M). As shown in Figure 3N, there was a more rapid decay of fluorescence in slices subjected to higher frequency, consistent with an increased number of synaptic vesicles that undergo fusion per action potential (Isaacson and Hille, 1997). We observed an increased fractional release when the same number of stimuli was applied at shorter interstimulus intervals, either as paired pulses or in burst-like stimuli (Figure 3O). These results indicate that higher rates of activity increase the probability of neurotransmitter release from D1R MSN synapses.

Effect of DA Denervation on Striatonigral Vesicular Fusion

We next examined whether DA lesions altered presynaptic activity. Brain slices were prepared from hypokinetic unilaterally 6-OHDA lesioned mice assessed by the corridor task 4 weeks after surgery. The rate of FM1-43 destaining in 6-OHDA lesioned mice ($t_{1/2}$ = 63.7 ± 7.1 s, n = 8 slices, 8 mice) was substantially faster than in sham animals ($t_{1/2}$ = 104.0 ± 5.7 s, n = 8 slices, 8 mice; $p < 0.001$, t test, Cohen's d = 2.22). There was a shift in the cumulative probability distribution (Figure 4C) of the $t_{1/2}$ of individual boutons to lower values in slices from lesioned mice ($p < 0.0001$, KS test, n = 183–219, 8 slices per group).

The density of active release sites was indistinguishable between sham and lesioned mice ($p > 0.05$, t test, Figure 4D). We likewise found no difference between the average fluorescence intensity of the individual synaptic boutons ($p > 0.05$, t test), or the amount of fluorescence (ΔF) lost during unloading ($p > 0.05$, t test). As FM1-43 loading depends on the number of synaptic vesicles that undergo recycling during stimulation (Harata et al., 2001), these data indicate that DA denervation enhances the release probability of the striatonigral pathway without altering the number of release sites or the total pool of recycling synaptic vesicles.

We tested whether DA denervation affected CB1R-mediated responses at the striatonigral synapses (Figure S8). We found no difference in the ability of CB1R ligands to modulate the $t_{1/2}$ of FM1-43 destaining between sham and 6-OHDA lesioned mice ($p > 0.05$, two-way ANOVA). These results suggest that the FM1-43 destaining is a measure of striatonigral activity in sham as well as in 6-OHDA mice.

We examined whether the effects of chronic DA lesion occurred following acute DA depletion by injecting mice with reserpine (5 mg/kg s.c.) 13 hr prior to slice preparation, which depletes >99% of striatal DA content (Bamford et al., 2004a). The kinetics of FM1-43 destaining in acutely DA depleted mice ($t_{1/2}$ = 116.3 ± 10.8, n = 10 slices, 10 mice) were not different from vehicle (0.1% acetic acid in 0.9% saline)-injected animals

(J) Frequency histogram (n = 665; 25 slices) of $t_{1/2}$ at 2 Hz with a theoretical gamma-function distribution (shape = 3.07, scale = 38.3, $p > 0.05$, KS-test) shown as a blue curve.

(K) FM1-43 destaining in control condition, with the CB1 agonist ACEA (10 μM), or the combination of the CB1 antagonist AM251 (10 μM) and ACEA.

(L) Box plot of CB1R-dependent effects on FM1-43 destaining. *$p < 0.05$ versus control, †††$p < 0.001$ versus ACEA (two-way ANOVA, Tukey's test).

(M) Pattern of stimulation used to examine frequency-dependent modulation of release probability. During FM1-43 unloading, stimulation was applied in trains, paired pulses (PP), or bursts. The final number of stimuli was identical (480 pulses) for each protocol.

(N) FM1-43 destaining from striatonigral terminals during stimuli delivered at 10 (blue diamonds, n = 321 boutons; 7 slices), 50 (red rectangles, n = 289 boutons; 7 slices), or 500 ms (black circles, n = 352 boutons; 7 slices) interstimulus duration.

(O) Box plot of fusion events per stimulus, fractional release (*f*). *$p < 0.05$, **$p < 0.01$ versus train (one-way ANOVA, Dunnett's test) (see also Figures S6 and S7).

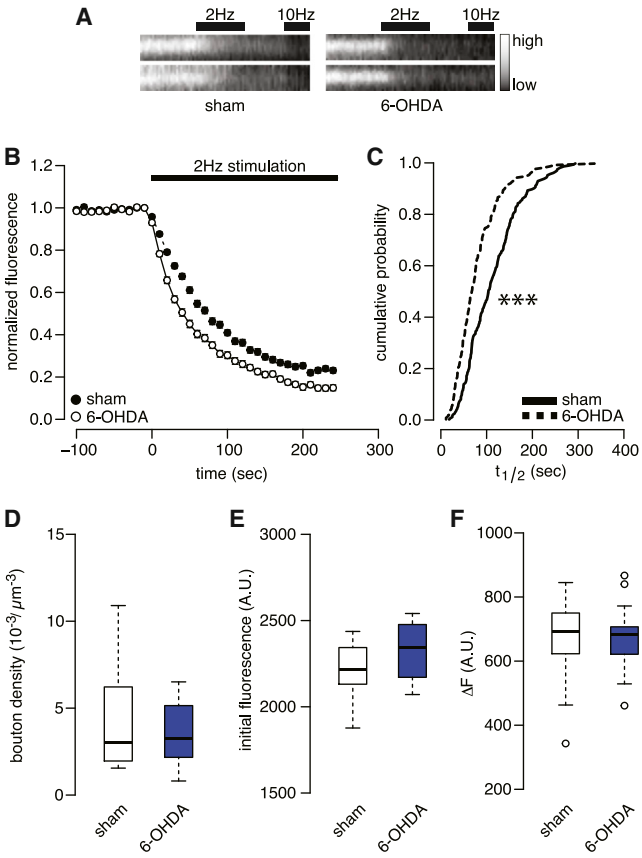

Figure 4. Increased Release Probability at Individual Striatonigral Synapses in 6-OHDA Lesioned Mice

(A) Micrographs of fluorescent boutons from the SNr of sham (left) and 6-OHDA lesioned (right) mice during unloading of FM1-43. Electrical stimulation was applied at indicated time and frequency (bars).

(B) Mean time course of FM1-43 destaining from striatonigral synapses in sham (n = 219 boutons, 8 slices) and 6-OHDA lesioned animals in ACSF (n = 183 boutons, 8 slices).

(C) Cumulative probability of the $t_{1/2}$ of FM1-43 destaining from individual striatonigral synapses of sham (black) and 6-OHDA-treated (blue) mice. ***p < 0.0001 versus sham (KS test).

(D–F) Box plots of (D) the density of active synaptic boutons per slice, as defined by FM1-43 destaining, (E) the fluorescence intensity of puncta before stimulation, and (F) the amount of fluorescence (ΔF) released during destaining. There were no differences (p > 0.05, t test) between sham (white) and 6-OHDA lesioned (blue) mice of the parameters presented in (D)–(F). Data are displayed as averages of each slice (see also Figure S8).

($t_{1/2}$ = 98.3 ± 6.8, n = 10 slices, 10 mice; p > 0.05; t test, data not shown). Thus, the increased striatonigral release probability observed in the 6-OHDA lesioned mice is an adaptation to long-term DA depletion.

Regulation of Striatonigral Vesicular Fusion by $GABA_B$ Receptors

What mechanism might be responsible for increased presynaptic striatonigral activity following long-term loss of DA? One possibility is that there is altered inhibition by presynaptic $GABA_B$ autoreceptors (Shen and Johnson, 1997). To test this hypothesis, the striatonigral synapses were labeled with FM1-43, and the $GABA_B$ antagonist CGP52432 (1 μM) was added during the unloading stimulus train. CGP52432 greatly enhanced the destaining rate of FM1-43 from striatonigral boutons in sham animals (Figure 5A). The cumulative distribution of the individual boutons of CGP52432-treated slices (p < 0.0001, KS test, n = 138–219, 6–8 slices) indicated that the majority of striatonigral synapses were inhibited by tonic $GABA_B$ signaling (Figure 5B).

In stark contrast, there was no effect of inhibiting $GABA_B$ receptors in the lesioned hemisphere of 6-OHDA-injected mice, and the distributions of $t_{1/2}$ values were nearly identical in untreated and CGP52432-treated slices (p > 0.05, KS-test, n = 183–201 boutons, 5–8 slices). While 6-OHDA lesioned mice showed faster destaining of striatonigral presynaptic sites, the stimulatory effect of $GABA_B$-receptor blockade was completely abolished (Figure 5E).

Together, these data suggest that the increased striatonigral release probability following DA lesion involves loss of tonic presynaptic $GABA_B$-mediated inhibition.

Regulation of Striatonigral Transmission by $GABA_B$ Receptors

To examine how presynaptic loss of $GABA_B$ inhibition affects striatonigral GABA transmission, we measured the effect of $GABA_B$ antagonism on electrically evoked outward $GABA_A$ currents in voltage-clamped SNr neurons (Figure 6A). Cesium was included in the pipette solution to minimize $GABA_B$-mediated postsynaptic effects through GIRK channels, and NBQX (10 μM) and AP5 (50 μM) were added to isolate $GABA_A$-receptor-mediated IPSCs.

In control slices, CGP52432 (1 μM) substantially increased the amplitude of the evoked IPSCs of sham animals (Figures 6B–6D). The antagonist increased the IPSCs elicited by the first (p < 0.05, t test) and second (p < 0.001, t test) pulse of paired-pulse stimuli (50 ms ITI). We found a larger increase (p < 0.01, t test) on the second eIPSC (25.2 ± 4.9 pA) than the first (11.4 ± 4.9 pA).

In striking contrast to controls, in slices from 6-OHDA lesioned mice, CGP52432 (1 μM) had no effect on the amplitude of either eIPSC of the paired pulse stimulus (Figures 6B, 6E, and 6F; first eIPSC, p > 0.05; second eIPSC, p > 0.05, t test).

These results suggest that normal presynaptic $GABA_B$-mediated inhibition of striatonigral release is abolished by DA denervation.

Effect of $GABA_B$ Receptor Stimulation on Striatonigral Release

To address how DA denervation alters $GABA_B$ function, we examined inhibition of FM1-43 unloading from sham-treated striatonigral synapses by the $GABA_B$ agonist, baclofen (1, 10 μM) (Figures 7A and 7B). In the presence of 10 μM baclofen, only a few puncta destained with 2 Hz stimuli; however, the same boutons displayed rapid synaptic vesicle fusion in response to 10 Hz stimuli. The effect of baclofen was blocked by preapplication of the $GABA_B$ antagonist CGP52432 (1 μM).

In DA lesioned mice, baclofen (1 μM) also inhibited synaptic vesicle exocytosis (Figure 7C), although the effect was substantially reduced. The number of active presynaptic sites

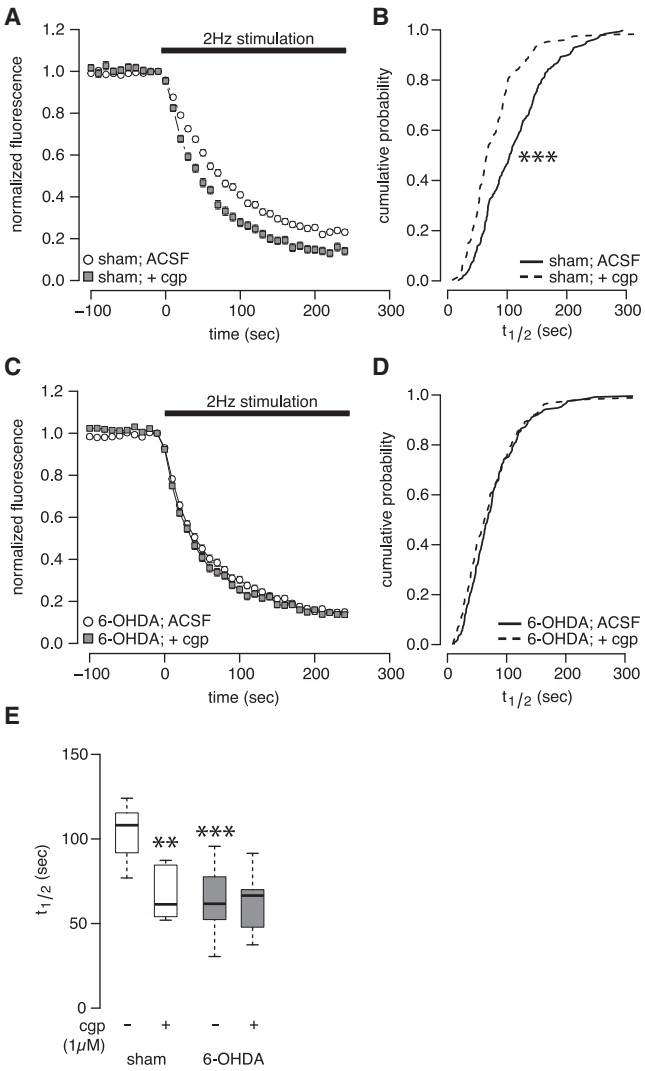

Figure 5. Reduced $GABA_B$ Mediated Tonic Inhibition of Vesicle Fusion at Striatonigral Synapses of 6-OHDA Lesioned Mice

(A) FM1-43 destaining from individual striatonigral synapses in slices from sham-treated mice in ACSF (circles, n = 219 boutons, 8 slices) or CGP52432 (cgp, 1 μM, squares, n = 138 boutons, 6 slices).

(B) Cumulative probability distribution of the $t_{1/2}$ of FM1-43 destaining from individual striatonigral synapses of sham-treated mice in ACSF (solid line) and in CGP52432 (dashed line). ***p < 0.0001 versus ACSF (KS test).

(C) FM1-43 destaining in 6-OHDA lesioned mice in ACSF (circles, n = 183 boutons, 8 slices) or with CGP52432 (1 μM, squares, n = 201 boutons, 5 slices).

(D) Cumulative probability distribution of the $t_{1/2}$ of FM1-43 destaining from striatonigral synapses in 6-OHDA lesioned mice in normal ACSF (solid line) or CGP52432 (1 μM).

(E) Box plot of mean FM1-43 destaining rates ($t_{1/2}$) in sham (white) and 6-OHDA lesioned mice, with or without CGP52432 (1 μM) during unloading. **p < 0.01, ***p < 0.001 versus sham ACSF (two-way ANOVA, Tukey's test).

(cf. Figure S7D) was identical in sham and DA-denervated slices (p > 0.05, one-way ANOVA). The fraction of boutons that responded to 2 Hz versus 10 Hz stimuli in baclofen was substantially higher in lesioned mice (Figures 7D and 7E), confirming decreased $GABA_B$ inhibition. The response to

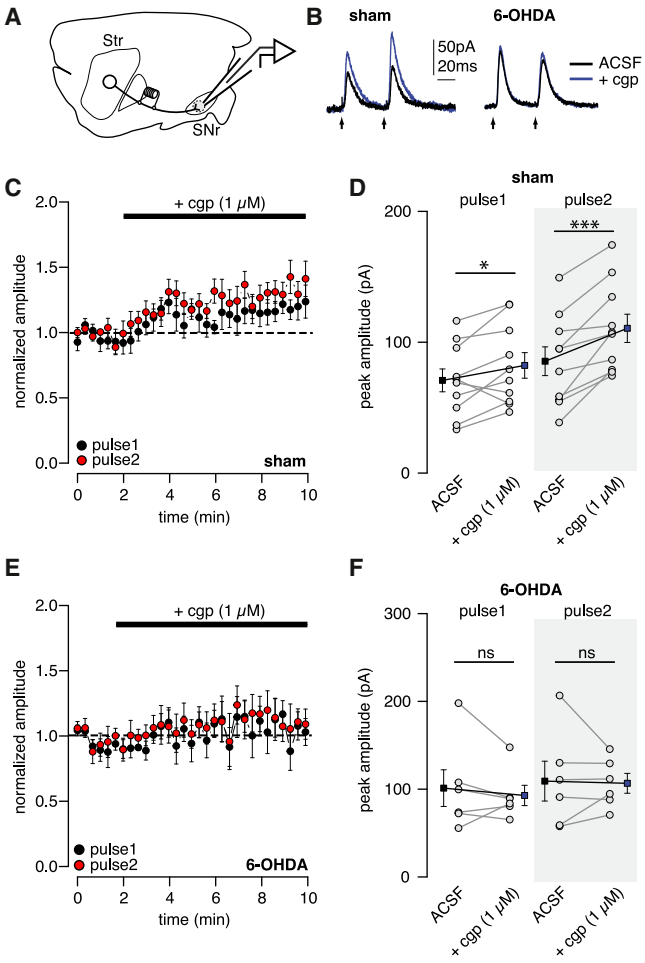

Figure 6. Reduced $GABA_B$ Mediated Tonic Inhibition of GABA Release in 6-OHDA Lesioned Mice

(A) Schematic of the sagittal slice preparation and positioning of the electrode used to evoke and record GABA release from striatonigral synapses.

(B) Evoked IPSCs recorded in voltage-clamped SNr neurons during baseline (black) and 10 min after application of CGP52432 (1 μM; blue) in sham (left) and 6-OHDA lesioned (right) mice.

(C–F) (C and E) Normalized IPSC peak amplitude of the first (black) and second (red) stimulus pulse during baseline and application of CGP52432 (1 μM) to slices from (C) sham and (E) 6-OHDA-treated mice. Mean IPSC peak current amplitude for pulse 1 and 2 in baseline condition and following application of CGP52432 (1 μM) are displayed for (D) sham and (F) 6-OHDA lesioned mice. Individual cells are displayed as gray circles, and the means (±SEM) for baseline (black) and CGP52432 (blue) are displayed as squares. ns, p > 0.05, *p < 0.05, ***p < 0.001 versus baseline (paired t test).

$GABA_B$ activation was, however, not absent in lesioned mice, as indicated by a significant reduction in destaining (Figure 7F). In addition, immunoblotting for $GABA_B$ receptors revealed no changes in $GABA_B$ receptor expression in the SNr on the DA denervated side compared to the intact side of the same animals (97% ± 7%, p > 0.05, t test; not shown). We conclude that tonic $GABA_B$-mediated inhibition of the striatonigral pathway is lost in the 6-OHDA lesioned mice, but that the $GABA_B$-receptor expression remains in the DA denervated SNr.

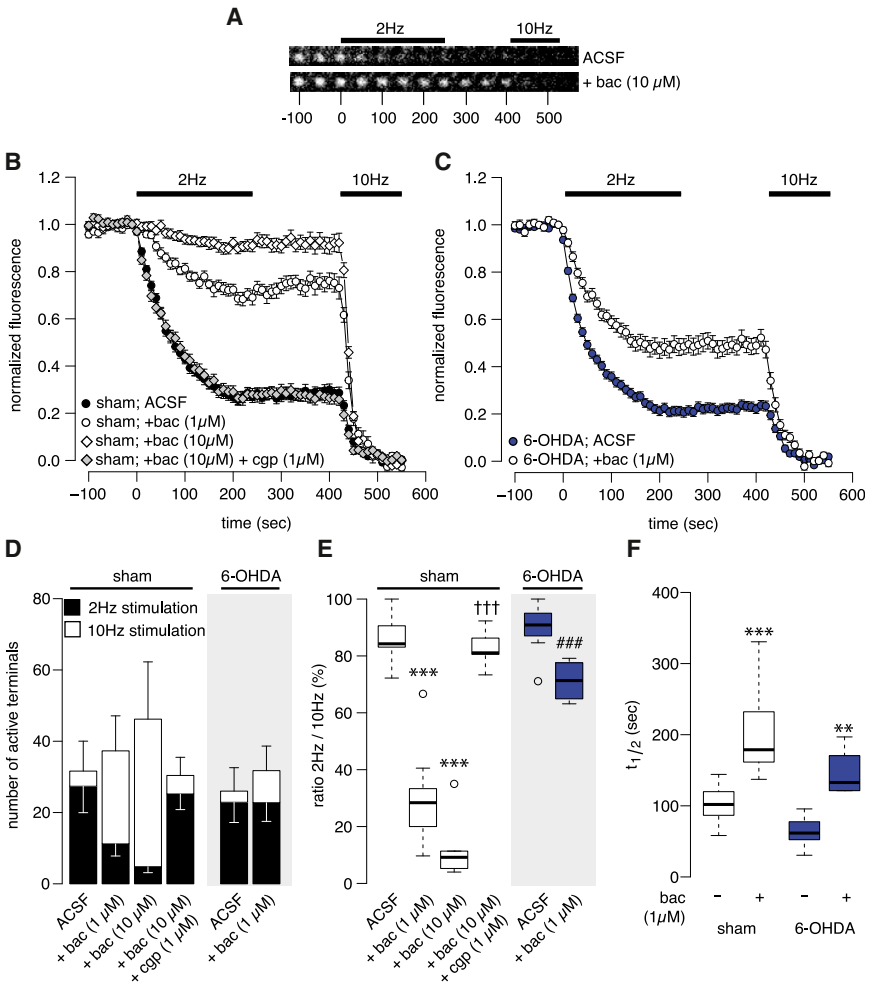

Figure 7. Inhibition of Synaptic Vesicle Fusion at Striatonigral Synapses by $GABA_B$ Receptors in Sham and 6-OHDA Lesioned Mice

(A) Two-photon micrographs of FM1-43-labeled synaptic boutons in a control slice (upper panel) and in a slice with baclofen (bac; 10 μM) added to the ACSF. Stimulation occurred at indicated intervals.

(B) FM1-43 destaining from striatonigral synapses in slices from sham mice, in control conditions (ACSF, black circles, n = 122 boutons, 5 slices) and in the presence of baclofen (1–10 μM, white circles and diamonds, n = 164–396 boutons; 5–11 slices) with or without CGP52432 (1 μM, gray diamonds, n = 138 boutons; 5 slices). Mean ± SEM.

(C) FM1-43 destaining from striatonigral synapses in slices from 6-OHDA mice in ACSF (blue circles, n = 203; 8 slices) and ACSF with baclofen (1 μM, n = 127 terminals, white circles, 4 slices). Mean ± SEM.

(D) Bar graph of the number of active terminals, as determined by FM1-43 unloading. The filled portion of the bars reports average number of boutons destaining in response to 2 Hz, and the open portion shows the average number of boutons that do not destain at 2 Hz but destain with subsequent 10 Hz stimuli. The bar height indicates the average number of active boutons per slice (±SEM). Baclofen (1, 10 μM) decreased the number of destaining synapses at 2 Hz, but a subsequent 10 Hz stimulus train revealed no difference in the total number of active boutons between groups ($p > 0.05$, one-way ANOVA).

(E) Box plot indicating the fraction of boutons destaining in response to 2 Hz unloading stimulation. Baclofen caused a decrease in the ratio of the boutons activated by 2 Hz that was occluded by CGP52432 (1 μM). With 1 μM baclofen, the ratio was higher in slices from 6-OHDA-treated mice. ***$p < 0.001$ versus ACSF, ††† $p < 0.001$ versus baclofen 10 μM, ###$p < 0.001$ versus sham baclofen 1 μM (two-way ANOVA, Tukey's test).

(F) Box plot of FM1-43 destaining rates ($t_{1/2}$) in control and baclofen-treated slices from sham and 6-OHDA mice during 2 Hz unloading stimulation. Baclofen decreased the release probability in sham as well as 6-OHDA lesioned mice. **$p < 0.01$, ***$p < 0.001$ versus ACSF (two-way ANOVA, Tukey's test).

DISCUSSION

Using selective optogenetic stimulation of striatonigral pathway synapses in vivo, we found that DA denervation sensitized striatonigral-mediated stimulation of motor activity in hemiparkinsonian mice. From optical and electrophysiological recordings of individual synapses within the SNr, we discovered that the behavioral abnormalities were associated with an increased GABA transmission in the striatonigral pathway that was due to a decreased presynaptic $GABA_B$ response. Thus, altered striatonigral synaptic activity plays an important role in parkinsonian symptoms and the sensitized responses that occur in PD therapy (Figure 8).

Our data reveal an increased excitability of the striatonigral synapse in DA lesioned mice, consistent with observations that D1R ligands administered into striatum (Fletcher and Starr, 1987) or SNr (Kozlowski and Marshall, 1980) induce more vigorous rotational behavior in DA lesioned than intact animals, and that intracerebral administration of DA is effective only following DA lesion (Fletcher and Starr, 1987). These effects are classically attributed to increased behavioral sensitivity to DA receptor stimulation (Schwarting and Huston, 1996). By selectively driving synaptic output of D1R MSNs using ChR2, we find, however, that DA denervated animals display increased contralateral rotational behavior via a mechanism independent of DA receptor stimulation. Importantly, this increased behavioral response occurred in animals that had no prior exposure to DA receptor ligands. We thus hypothesize that while hypoactivity of D1R MSNs observed in vivo is due to loss of D1R-mediated modulation of striatonigral MSN activity (Mallet et al., 2006), reduced $GABA_B$-mediated presynaptic inhibition results in striatonigral facilitation and increased GABA release during synaptic activity (Figure 8). To our knowledge, this provides a first direct demonstration of a compensatory increase in striatonigral synaptic activity in parkinsonian conditions that is independent of DA receptor activation.

D1R MSN activation can elicit antiparkinsonian (Kravitz et al., 2010), reinforcing (Kravitz et al., 2012) and rewarding responses

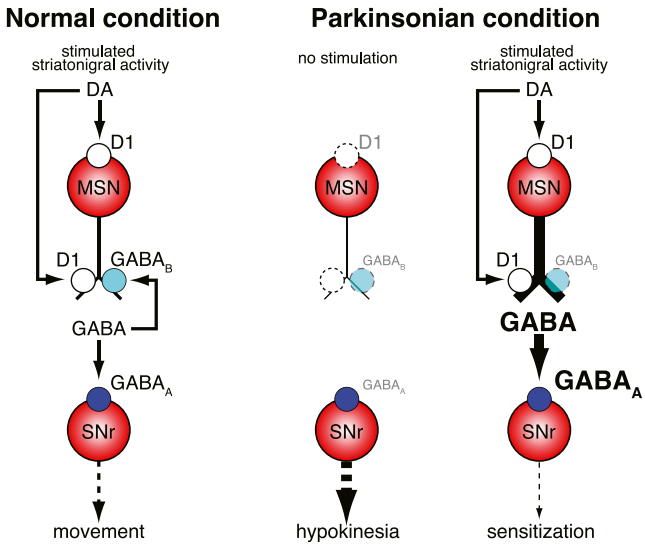

Figure 8. Striatonigral Mediated Motor Sensitization in PD

In normal intact brain (left panel), stimulation of the striatonigral MSNs in the presence of D1R agonists including DA provides normal GABA release in the SNr, which activates postsynaptic $GABA_A$ receptors and inhibits SNr firing. This disinhibits thalamocortical synapses and triggers the initiation of movement. At the striatonigral synapse, GABA also inhibits release from striatonigral synapses via presynaptic $GABA_B$ receptors. Together, postsynaptic $GABA_A$ and presynaptic $GABA_B$ activation define the kinetics of striatonigral control of SNr outputs and enable appropriate selection of motor behaviors. In the parkinsonian brain (right panels), midbrain DA neurons have degenerated and DA is not available to regulate striatonigral activity. This leads to atypical firing patterns in SNr and causes motor disabilities. Furthermore, the presynaptic inhibition of striatonigral release by $GABA_B$ receptors is lost, disrupting the normal control of SNr activity. As a consequence, when striatonigral synapses are stimulated, an abnormally high level of GABA release is triggered, leading to sustained inhibition and changes in firing patterns of SNr neurons. This results in a sensitized motor response that may produce the undesired side effects of L-DOPA therapy in PD.

(Ferguson et al., 2011; Hikida et al., 2010). Here, we find that stimulation of GABA release from the striatonigral synapse reduces parkinsonism, suggesting that both striatal and nigral activation of the striatonigral pathway restore motor activity in DA denervated animals. Striatonigral and striatopallidal MSNs are associated by reciprocal axon collaterals (Tunstall et al., 2002) that are modulated by DA (Guzmán et al., 2003) and dysregulated in PD models (Taverna et al., 2008), and maintain synaptic connections with cholinergic interneurons (Chuhma et al., 2011) that may modulate striatal output activity via MSNs, and GABAergic interneurons (English et al., 2012). Thus, selective stimulation of striatal neurons can affect behavior via complex networks, a feature of less concern in the SNr, where the striatonigral synapses directly influence basal ganglia output. In support of local action of the optogenetic stimulation applied to the striatonigral efferents, we observed no activation of c-Fos in the striatum. We thus demonstrate that selective stimulation of the D1R MSNs synapses in SNr can drive behavior, suggesting that local pharmacological manipulation of these presynaptic sites may correct the hypokinetic symptoms of PD.

To directly measure presynaptic striatonigral activity, we adapted an optical approach previously developed to examine individual Schaffer collateral hippocampal (Zakharenko et al., 2001) and corticostriatal synapses (Bamford et al., 2004b) using an endocytic fluorescent probe, FM1-43, that measures synaptic vesicle exocytosis (Betz and Bewick, 1992). FM1-43 unloading from D1R expressing MSN axon terminals was dependent on intact connections from the rostral forebrain to the SNr (Figure S7), on Ca^{2+} influx (Figure S6), and was inhibited by CB1R that are specifically expressed by striatonigral efferents (Figures 3 and S8). In addition, FM1-43 unloading displayed the same features of short-term plasticity as in electrophysiological recordings of SNr neurons, including PPF (Figure 3).

The selective FM1-43 labeling of striatonigral synapses was unexpected, since stimulation of the descending fibers appeared to activate pallidonigral efferents and SNr neurons have tonically active axon collaterals (Rick and Lacey, 1994). The apparent lack of significant label at those sites may be because the labeled synaptic vesicles undergo exocytosis during the wash period (>20 min). Furthermore, FM1-43-labeled boutons did not form visible contact with cell bodies. This pattern of labeled synapses is consistent with the organization of striatonigral efferents, which provide small synaptic contacts with fine distal dendrites of SNr projection neurons, in contrast to pallidonigral inputs that make large basket-shaped synapses on proximal dendrites and soma (von Krosigk et al., 1992).

The increased striatonigral function in DA denervated animals was not reproduced by reserpine, indicating that the synaptic plasticity results from long-term loss of DA signaling. In the DA intact brain, the striatonigral pathway is controlled by D1Rs on direct pathway MSNs dendrites as well as on axon terminals within the SNr (Altar and Hauser, 1987). The coupling of the D1R to the adenylyl cyclase/protein kinase A/DARPP-32 cascade permits widespread effects on neuronal excitability and subsequent neurotransmitter release (Svenningsson et al., 2004) that may account for the DA receptor-independent effects observed in our study. Indeed, DA depletion changes the gene expression of voltage-gated potassium and VGCC (Meurers et al., 2009), providing molecular links to the increased excitability of D1R MSN (Fieblinger et al., 2014; Warre et al., 2011) and increased GABA release at the striatonigral synapse. The SNr may act as a central locus for denervation-induced changes, leading to sensitization to L-DOPA. Homeostatic changes can exist in SNr neurons controlled by D1/5 heteroreceptors (Zhou et al., 2009). Exaggerated effects of DA would be expected when feedback regulation of extracellular DA via D2R and DAT expressed by SNc dendrites in the SNr are lost. Indeed, rotational behavior to L-DOPA in 6-OHDA-injected rats is decreased by local administration of D1R antagonists to the SNr (Robertson and Robertson, 1989), and the in vivo DA levels produced by L-DOPA are higher in the SNr of lesioned than intact animals (Lindgren et al., 2010). Our experiments did not reveal changes in the firing properties of SNr neurons, which suggests that GABA release from axon collaterals of SNr neurons is unaffected by the DA denervation itself. Differences in GABA release could appear in response to D1R stimulation, however, as indicated by the ability of D1R agonists to increase the frequency of sIPSCs in SNr cells of 6-OHDA-treated mice (Mango et al., 2014).

While electrophysiology and imaging experiments demonstrated a reduced $GABA_B$-mediated control of GABA release in DA denervated animals, no lesion-induced alterations in $GABA_B$ receptor expression were found. The effects on $GABA_B$ receptor function may occur at the coupling to G-proteins and/or second messenger signaling, including increased expression of G_{olf} (Corvol et al., 2004), adenylyl cyclase V/VI (Rangel-Barajas et al., 2011), or reduced phosphodiesterase-mediated hydrolysis of cAMP (Mango et al., 2014). Consistently, GABA release in the SNr is enhanced by the adenylyl cyclase activator, forskolin (Radnikow and Misgeld, 1998). Alternatively, decreased $GABA_B$ function could arise from altered interactions of $G\beta\gamma$ and N-, P/Q-type VGCC, a mechanism by which $GABA_B$ receptors inhibit neurotransmitter release (Bettler and Tiao, 2006). A role for a VGCC-dependent mechanism is consistent with our observation that inhibition of vesicular fusion by baclofen was overcome at higher frequencies of synaptic activity (10 Hz; cf. Figure 7). A similar phenomenon at hippocampal synapses (Isaacson and Hille, 1997) was attributed to a dissociation of the $G\beta\gamma$ complex from its binding to VGCC during strong synaptic stimulation. Future studies will be required to fully characterize the molecular mechanisms by which $GABA_B$ receptors control GABA release in normal and DA-denervated SNr.

The goal of current symptomatic therapies for PD is to restore DA function within the striatum. In contrast, our data indicate that antiparkinsonian effects and the expression of sensitization, classically considered DA-mediated responses, can be achieved independently from DA receptor activation by modulation of the striatonigral pathway within the SNr. These findings suggest that future PD therapeutics might be aimed at controlling the activity of SNr neurons. Increased stimulus-dependent activity of the striatonigral pathway may represent a mechanism whereby L-DOPA causes dyskinesias, impulse control disorders, or DA dysregulation syndrome in PD patients. If so, treatments re-establishing appropriate presynaptic modulation GABA release at the striatonigral synapse may be clinically beneficial. Our findings suggest that strategies that restore tonic inhibition via $GABA_B$ receptors or stimulation of CB1R may reduce adverse effects of L-DOPA in the treatment of PD.

EXPERIMENTAL PROCEDURES

All experiments were approved by the Institutional Animal Care and Use Committee (IACUC) at the Columbia University. Unilateral injections of 6-OHDA or vehicle, and adeno-associated viruses carrying the genes for ChR2 and eYFP proteins, were performed by craniotomy in adult BAC-D1 mice or C57Bl/6J mice. Experiments were carried out 3–4 weeks after surgery. All 6-OHDA-treated mice were tested for DA-denervation-induced parkinsonian symptoms using the corridor test. For optogenetic control of motor behavior, blue light (473 nm, 10 mW) was delivered through an optic fiber implanted into the SNr.

Sagittal brain slices were prepared from DA-depleted and sham control mice and incubated for 15 min in ACSF containing FM1-43 (10 μM), NBQX (10 μM), and AP-5 (50 μM). Striatonigral fibers were then stimulated 5 min at 10 Hz to incorporate FM1-43 into recycling synaptic vesicles (Figure 3). To provide full labeling of the recycling vesicles, FM1-43 was present for 1 min after the loading stimulus. The same loading protocol was applied throughout the study. Following wash with ACSF containing ADVASEP-7 (100 μM, Biotium), the fusion of FM1-43-labeled vesicles in SNr was measured during a second electrical stimulus of variable frequencies (1–10 Hz) in the same position. Finally, following 3 min of inactivity, the synapses were subjected to 10 Hz stimuli for 2 min to deplete any pool of remaining labeled vesicles.

Statistical analysis and full methods including behavior analysis, description of solutions, equipment, and recording procedures for FM1-43 destaining and patch clamp electrophysiology can be found in Supplemental Experimental Procedures.

SUPPLEMENTAL INFORMATION

Supplemental Information includes eight figures, three tables, three movies, and Supplemental Experimental Procedures and can be found with this article at http://dx.doi.org/10.1016/j.neuron.2015.08.022.

AUTHOR CONTRIBUTIONS

D.S. directed the study, and A.B. and D.S. conceived and designed the study. A.B. performed surgery, behavior experiments, two-photon imaging, and patch-clamp electrophysiology; developed routines for data analysis; and analyzed data. E.M.A. performed cell-attached recordings. M.Y.W. performed biochemical experiments. M.A.K. designed research and provided expertise on optogenetics. M.S.S. designed research and assisted A.B. on two-photon imaging and image data analysis. R.H. contributed with reagents and materials for optogenetics. The manuscript was written by A.B. and D.S. and edited by all authors.

ACKNOWLEDGMENTS

This work was supported by the JPB and Parkinson's Disease Foundations, NIH NIDA10154, and the Udall Center of Excellence for Parkinson's Disease research at Columbia University. A.B. received fellowships from the Swedish Research Council and Sweden-America Foundation. We thank Karl Deisseroth for the ChR2 plasmid; Drs. Neil Harrison, Sejoon Choi, and Ana Mrejeru for advice on patch clamp experiments; and Nigel Bamford for advice on two-photon imaging. We thank Drs. Un Kang, Carolina Cebrian, Eugene Mosharov, and Emanuela Santini for discussion and critical review, and Candace Castagna and Vanessa Morales for excellent animal care.

Received: July 2, 2014
Revised: May 14, 2015
Accepted: August 12, 2015
Published: September 2, 2015

REFERENCES

Altar, C.A., and Hauser, K. (1987). Topography of substantia nigra innervation by D1 receptor-containing striatal neurons. Brain Res. *410*, 1–11.

Bamford, N.S., Robinson, S., Palmiter, R.D., Joyce, J.A., Moore, C., and Meshul, C.K. (2004a). Dopamine modulates release from corticostriatal terminals. J. Neurosci. *24*, 9541–9552.

Bamford, N.S., Zhang, H., Schmitz, Y., Wu, N.P., Cepeda, C., Levine, M.S., Schmauss, C., Zakharenko, S.S., Zablow, L., and Sulzer, D. (2004b). Heterosynaptic dopamine neurotransmission selects sets of corticostriatal terminals. Neuron *42*, 653–663.

Bettler, B., and Tiao, J.Y. (2006). Molecular diversity, trafficking and subcellular localization of GABAB receptors. Pharmacol. Ther. *110*, 533–543.

Betz, W.J., and Bewick, G.S. (1992). Optical analysis of synaptic vesicle recycling at the frog neuromuscular junction. Science *255*, 200–203.

Chuhma, N., Tanaka, K.F., Hen, R., and Rayport, S. (2011). Functional connectome of the striatal medium spiny neuron. J. Neurosci. *31*, 1183–1192.

Connelly, W.M., Schulz, J.M., Lees, G., and Reynolds, J.N. (2010). Differential short-term plasticity at convergent inhibitory synapses to the substantia nigra pars reticulata. J. Neurosci. *30*, 14854–14861.

Corvol, J.C., Muriel, M.P., Valjent, E., Féger, J., Hanoun, N., Girault, J.A., Hirsch, E.C., and Hervé, D. (2004). Persistent increase in olfactory type

G-protein alpha subunit levels may underlie D1 receptor functional hypersensitivity in Parkinson disease. J. Neurosci. *24*, 7007–7014.

Deniau, J.M., Kitai, S.T., Donoghue, J.P., and Grofova, I. (1982). Neuronal interactions in the substantia nigra pars reticulata through axon collaterals of the projection neurons. An electrophysiological and morphological study. Exp. Brain Res. *47*, 105–113.

Deniau, J.M., Mailly, P., Maurice, N., and Charpier, S. (2007). The pars reticulata of the substantia nigra: a window to basal ganglia output. Prog. Brain Res. *160*, 151–172.

English, D.F., Ibanez-Sandoval, O., Stark, E., Tecuapetla, F., Buzsáki, G., Deisseroth, K., Tepper, J.M., and Koos, T. (2012). GABAergic circuits mediate the reinforcement-related signals of striatal cholinergic interneurons. Nat. Neurosci. *15*, 123–130.

Fahn, S. (2000). The spectrum of levodopa-induced dyskinesias. Ann. Neurol. *47*, S2–S9, discussion S9–S11.

Ferguson, S.M., Eskenazi, D., Ishikawa, M., Wanat, M.J., Phillips, P.E., Dong, Y., Roth, B.L., and Neumaier, J.F. (2011). Transient neuronal inhibition reveals opposing roles of indirect and direct pathways in sensitization. Nat. Neurosci. *14*, 22–24.

Feyder, M., Bonito-Oliva, A., and Fisone, G. (2011). L-DOPA-induced dyskinesia and abnormal signaling in striatal medium spiny neurons: focus on dopamine D1 receptor-mediated transmission. Front. Behav. Neurosci. *5*, 71.

Fieblinger, T., Graves, S.M., Sebel, L.E., Alcacer, C., Plotkin, J.L., Gertler, T.S., Chan, C.S., Heiman, M., Greengard, P., Cenci, M.A., and Surmeier, D.J. (2014). Cell type-specific plasticity of striatal projection neurons in parkinsonism and L-DOPA-induced dyskinesia. Nat. Commun. *5*, 5316.

Fletcher, G.H., and Starr, M.S. (1987). Topography of dopamine behaviours mediated by D1 and D2 receptors revealed by intrastriatal injection of SKF 38393, lisuride and apomorphine in rats with a unilateral 6-hydroxydopamine-induced lesion. Neuroscience *20*, 589–597.

Gerfen, C.R. (1992). The neostriatal mosaic: multiple levels of compartmental organization. Trends Neurosci. *15*, 133–139.

Gerfen, C.R., Engber, T.M., Mahan, L.C., Susel, Z., Chase, T.N., Monsma, F.J., Jr., and Sibley, D.R. (1990). D1 and D2 dopamine receptor-regulated gene expression of striatonigral and striatopallidal neurons. Science *250*, 1429–1432.

Grealish, S., Mattsson, B., Draxler, P., and Björklund, A. (2010). Characterisation of behavioural and neurodegenerative changes induced by intranigral 6-hydroxydopamine lesions in a mouse model of Parkinson's disease. Eur. J. Neurosci. *31*, 2266–2278.

Guzmán, J.N., Hernández, A., Galarraga, E., Tapia, D., Laville, A., Vergara, R., Aceves, J., and Bargas, J. (2003). Dopaminergic modulation of axon collaterals interconnecting spiny neurons of the rat striatum. J. Neurosci. *23*, 8931–8940.

Harata, N., Ryan, T.A., Smith, S.J., Buchanan, J., and Tsien, R.W. (2001). Visualizing recycling synaptic vesicles in hippocampal neurons by FM 1-43 photoconversion. Proc. Natl. Acad. Sci. USA *98*, 12748–12753.

Hikida, T., Kimura, K., Wada, N., Funabiki, K., and Nakanishi, S. (2010). Distinct roles of synaptic transmission in direct and indirect striatal pathways to reward and aversive behavior. Neuron *66*, 896–907.

Isaacson, J.S., and Hille, B. (1997). GABA(B)-mediated presynaptic inhibition of excitatory transmission and synaptic vesicle dynamics in cultured hippocampal neurons. Neuron *18*, 143–152.

Jackman, S.L., Beneduce, B.M., Drew, I.R., and Regehr, W.G. (2014). Achieving high-frequency optical control of synaptic transmission. J. Neurosci. *34*, 7704–7714.

Kay, A.R., Alfonso, A., Alford, S., Cline, H.T., Holgado, A.M., Sakmann, B., Snitsarev, V.A., Stricker, T.P., Takahashi, M., and Wu, L.G. (1999). Imaging synaptic activity in intact brain and slices with FM1-43 in C. elegans, lamprey, and rat. Neuron *24*, 809–817.

Kozlowski, M.R., and Marshall, J.F. (1980). Rotation induced by intranigral injections of GABA agonists and antagonists: zone-specific effects. Pharmacol. Biochem. Behav. *13*, 561–567.

Kravitz, A.V., Freeze, B.S., Parker, P.R., Kay, K., Thwin, M.T., Deisseroth, K., and Kreitzer, A.C. (2010). Regulation of parkinsonian motor behaviours by optogenetic control of basal ganglia circuitry. Nature *466*, 622–626.

Kravitz, A.V., Tye, L.D., and Kreitzer, A.C. (2012). Distinct roles for direct and indirect pathway striatal neurons in reinforcement. Nat. Neurosci. *15*, 816–818.

Langston, J.W., and Ballard, P. (1984). Parkinsonism induced by 1-methyl-4-phenyl-1,2,3,6-tetrahydropyridine (MPTP): implications for treatment and the pathogenesis of Parkinson's disease. Can. J. Neurol. Sci. *11* (1, Suppl), 160–165.

Lindgren, H.S., Andersson, D.R., Lagerkvist, S., Nissbrandt, H., and Cenci, M.A. (2010). L-DOPA-induced dopamine efflux in the striatum and the substantia nigra in a rat model of Parkinson's disease: temporal and quantitative relationship to the expression of dyskinesia. J. Neurochem. *112*, 1465–1476.

Mallet, N., Ballion, B., Le Moine, C., and Gonon, F. (2006). Cortical inputs and GABA interneurons imbalance projection neurons in the striatum of parkinsonian rats. J. Neurosci. *26*, 3875–3884.

Mango, D., Bonito-Oliva, A., Ledonne, A., Nistico, R., Castelli, V., Giorgi, M., Sancesario, G., Fisone, G., Berretta, N., and Mercuri, N.B. (2014). Phosphodiesterase 10A controls D1-mediated facilitation of GABA release from striato-nigral projections under normal and dopamine-depleted conditions. Neuropharmacology *76*, 127–136.

Marshall, J.F., and Ungerstedt, U. (1977). Supersensitivity to apomorphine following destruction of the ascending dopamine neurons: quantification using the rotational model. Eur. J. Pharmacol. *41*, 361–367.

Mátyás, F., Yanovsky, Y., Mackie, K., Kelsch, W., Misgeld, U., and Freund, T.F. (2006). Subcellular localization of type 1 cannabinoid receptors in the rat basal ganglia. Neuroscience *137*, 337–361.

Meurers, B.H., Dziewczapolski, G., Shi, T., Bittner, A., Kamme, F., and Shults, C.W. (2009). Dopamine depletion induces distinct compensatory gene expression changes in DARPP-32 signal transduction cascades of striatonigral and striatopallidal neurons. J. Neurosci. *29*, 6828–6839.

Miyazaki, T., and Lacey, M.G. (1998). Presynaptic inhibition by dopamine of a discrete component of GABA release in rat substantia nigra pars reticulata. J. Physiol. *513*, 805–817.

Morelli, M., Fenu, S., Garau, L., and Di Chiara, G. (1989). Time and dose dependence of the 'priming' of the expression of dopamine receptor supersensitivity. Eur. J. Pharmacol. *162*, 329–335.

Nadjar, A., Gerfen, C.R., and Bezard, E. (2009). Priming for l-dopa-induced dyskinesia in Parkinson's disease: a feature inherent to the treatment or the disease? Prog. Neurobiol. *87*, 1–9.

Pons, R., Syrengelas, D., Youroukos, S., Orfanou, I., Dinopoulos, A., Cormand, B., Ormazabal, A., Garzía-Cazorla, A., Serrano, M., and Artuch, R. (2013). Levodopa-induced dyskinesias in tyrosine hydroxylase deficiency. Mov. Disord. *28*, 1058–1063.

Putterman, D.B., Munhall, A.C., Kozell, L.B., Belknap, J.K., and Johnson, S.W. (2007). Evaluation of levodopa dose and magnitude of dopamine depletion as risk factors for levodopa-induced dyskinesia in a rat model of Parkinson's disease. J. Pharmacol. Exp. Ther. *323*, 277–284.

Radnikow, G., and Misgeld, U. (1998). Dopamine D1 receptors facilitate GABAA synaptic currents in the rat substantia nigra pars reticulata. J. Neurosci. *18*, 2009–2016.

Rangel-Barajas, C., Silva, I., García-Ramírez, M., Sánchez-Lemus, E., Floran, L., Aceves, J., Erlij, D., and Florán, B. (2008). 6-OHDA-induced hemiparkinsonism and chronic L-DOPA treatment increase dopamine D1-stimulated [(3)H]-GABA release and [(3)H]-cAMP production in substantia nigra pars reticulata of the rat. Neuropharmacology *55*, 704–711.

Rangel-Barajas, C., Silva, I., Lopéz-Santiago, L.M., Aceves, J., Erlij, D., and Florán, B. (2011). L-DOPA-induced dyskinesia in hemiparkinsonian rats is associated with up-regulation of adenylyl cyclase type V/VI and increased GABA release in the substantia nigra reticulata. Neurobiol. Dis. *41*, 51–61.

Rick, C.E., and Lacey, M.G. (1994). Rat substantia nigra pars reticulata neurones are tonically inhibited via GABAA, but not GABAB, receptors in vitro. Brain Res. *659*, 133–137.

Robertson, G.S., and Robertson, H.A. (1989). Evidence that L-dopa-induced rotational behavior is dependent on both striatal and nigral mechanisms. J. Neurosci. *9*, 3326–3331.

Romo-Parra, H., Misgeld, U., and Yanovsky, Y. (2009). Regular firing of a single output neuron reduces its own inhibition through endocannabinoids in substantia nigra pars reticulata of juvenile mice. Neuroscience *160*, 596–605.

Schwarting, R.K., and Huston, J.P. (1996). Unilateral 6-hydroxydopamine lesions of meso-striatal dopamine neurons and their physiological sequelae. Prog. Neurobiol. *49*, 215–266.

Shen, K.Z., and Johnson, S.W. (1997). Presynaptic GABAB and adenosine A1 receptors regulate synaptic transmission to rat substantia nigra reticulata neurones. J. Physiol. *505*, 153–163.

Svenningsson, P., Nishi, A., Fisone, G., Girault, J.A., Nairn, A.C., and Greengard, P. (2004). DARPP-32: an integrator of neurotransmission. Annu. Rev. Pharmacol. Toxicol. *44*, 269–296.

Taverna, S., Ilijic, E., and Surmeier, D.J. (2008). Recurrent collateral connections of striatal medium spiny neurons are disrupted in models of Parkinson's disease. J. Neurosci. *28*, 5504–5512.

Tunstall, M.J., Oorschot, D.E., Kean, A., and Wickens, J.R. (2002). Inhibitory interactions between spiny projection neurons in the rat striatum. J. Neurophysiol. *88*, 1263–1269.

von Krosigk, M., Smith, Y., Bolam, J.P., and Smith, A.D. (1992). Synaptic organization of GABAergic inputs from the striatum and the globus pallidus onto neurons in the substantia nigra and retrorubral field which project to the medullary reticular formation. Neuroscience *50*, 531–549.

Voon, V., Mehta, A.R., and Hallett, M. (2011). Impulse control disorders in Parkinson's disease: recent advances. Curr. Opin. Neurol. *24*, 324–330.

Waddington, J.L., and Cross, A.J. (1979). Baclofen and muscimol: behavioural and neurochemical sequelae of unilateral intranigral administration and effects on 3H-GABA receptor binding. Naunyn Schmiedebergs Arch. Pharmacol. *306*, 275–280.

Wallmichrath, I., and Szabo, B. (2002). Cannabinoids inhibit striatonigral GABAergic neurotransmission in the mouse. Neuroscience *113*, 671–682.

Warre, R., Thiele, S., Talwar, S., Kamal, M., Johnston, T.H., Wang, S., Lam, D., Lo, C., Khademullah, C.S., Perera, G., et al. (2011). Altered function of glutamatergic cortico-striatal synapses causes output pathway abnormalities in a chronic model of parkinsonism. Neurobiol. Dis. *41*, 591–604.

Weintraub, D., and Nirenberg, M.J. (2013). Impulse control and related disorders in Parkinson's disease. Neurodegener. Dis. *11*, 63–71.

Zakharenko, S.S., Zablow, L., and Siegelbaum, S.A. (2001). Visualization of changes in presynaptic function during long-term synaptic plasticity. Nat. Neurosci. *4*, 711–717.

Zhang, Y.P., and Oertner, T.G. (2007). Optical induction of synaptic plasticity using a light-sensitive channel. Nat. Methods *4*, 139–141.

Zhou, F.W., Jin, Y., Matta, S.G., Xu, M., and Zhou, F.M. (2009). An ultra-short dopamine pathway regulates basal ganglia output. J. Neurosci. *29*, 10424–10435.

Zucker, R.S., and Regehr, W.G. (2002). Short-term synaptic plasticity. Annu. Rev. Physiol. *64*, 355–405.